

Raman scattering by acoustic phonons in Fibonacci GaAs-AlAs superlattices

K. Bajema and R. Merlin

Department of Physics, The University of Michigan, Ann Arbor, Michigan 48109-1120

(Received 23 June 1987)

We report on resonant and nonresonant Raman scattering by acoustic phonons in Fibonacci GaAs-AlAs superlattices. Spectra off resonance are dominated by doublets centered at frequencies that follow a power-law behavior, in good agreement with numerical calculations based on a continuum model. Resonant data show a weighted density of states revealing the expected rich structure of gaps in the phonon spectrum. It is proposed that the electronic excitation involved in the resonant process is an intrinsic surface state of the superlattice.

Layered structures (superlattices) based on the Fibonacci sequence exhibit quasiperiodicity with two lengths that are in a ratio given by the golden mean $\tau = (1 + \sqrt{5})/2$.^{1,2} The properties of these artificial materials, closely related to one-dimensional (1D) quasicrystals,³ have been extensively discussed in recent experimental^{1,2,4,5} and theoretical⁶⁻¹⁹ studies. In this Rapid Communication, we report a Raman scattering (RS) investigation of longitudinal-acoustic (LA) phonons in GaAs-AlAs Fibonacci superlattices (FSL's). The spectra provide separate information on (i) the superlattice structure factor (as with the "folded" phonons of the periodic case)²⁰ and (ii) the frequency spectrum of LA modes, depending on the excitation energy ω_L . Specifically, the expected hierarchical structure of gaps in the 1D density of states^{8,12,15,19} is revealed by *resonant* data; *off-resonant* spectra exhibit phonon doublets that follow a power-law behavior reflecting the self-similarity^{1-3,14,18} of the reciprocal lattice. The latter findings are shown to be consistent with previous x-ray measurements.² We further present results of continuum-model calculations which support our interpretation.

The FSL used in this work has been described previously.^{1,2} It corresponds to generation 13 of the Fibonacci sequence (377 elements), and it was grown by molecular-beam epitaxy on (001) GaAs. The two building blocks are $A \equiv [17\text{-\AA AlAs}-42\text{-\AA GaAs}]$ and $B \equiv [17\text{-\AA AlAs}-20\text{-\AA GaAs}]$. Raman spectra were recorded in the $z(x',x')\bar{z}$ backscattering configuration where z is normal to the layers and x' is along the [110] direction. In the acoustic region, this geometry only allows scattering by LA phonons with wave vectors parallel to [001].²⁰ As excitation sources we used the discrete lines of Kr^+ and Ar^+ lasers, and a DCM (4-dicyanomethylene-2-methyl-6-*p*-dimethyl-aminostyryl-4*H*-piran) dye laser. Data were obtained at $T = 300$ K with power densities in the range 50–100 W cm^{-2} .

In the calculations, the displacement pattern $u(z)$ and the frequency Ω of [001] LA modes were obtained by numerically solving the wave equation

$$-\Omega^2 u = c^2(z) (d^2 u / dz^2), \quad (1)$$

valid for piecewise-constant modulations. The LA sound velocity is $c(z) = c_n$ in layer n . The scattering intensity

was determined from the continuum-model expression:²⁰

$$I(\Omega) \propto \left| \sum_k (q-k) P_k u_{q-k} \right|^2 [n(\Omega) + 1] / \Omega, \quad (2)$$

where u_{q-k} is the corresponding (normalized) Fourier component of the amplitude of the phonon with frequency Ω , $n(\Omega)$ is the Bose factor, P_k is the Fourier transform of the photoelastic coefficient $p^{12}(z) = p_n^{12}$ in the n th layer, and q is the scattering wave vector.

Figure 1 shows Raman spectra of the FSL for two laser energies ω_L . The top and bottom spectra correspond, respectively, to resonant and nonresonant conditions; as shown by the reflectivity data in the inset, $\omega_L = 1.916$ eV is close to a critical point for optical transitions (at ~ 1.89 eV), while $\omega_L = 2.409$ eV falls in a relatively featureless

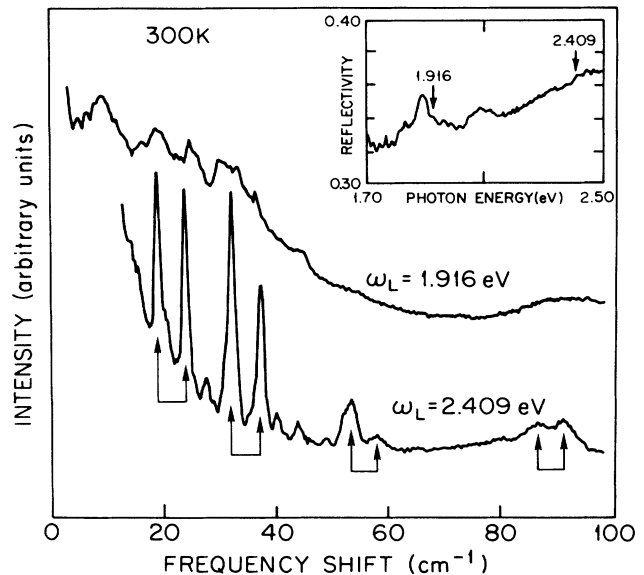


FIG. 1. Typical resonant ($\omega_L = 1.916$ eV) and nonresonant ($\omega_L = 2.409$ eV) Raman spectra of the Fibonacci superlattice showing LA scattering. Arrows indicate principle doublets. The scattering geometry is $z(x',x')\bar{z}$. Inset: normal reflectivity data. The scattering resonance is due to the electronic transition associated with the peak at ~ 1.89 eV.

region of the spectrum. The differences between resonant and off-resonance results are striking. The former exhibit a complex line shape with “dips” that are ascribed to gaps in the LA density of states (see below). Within experimental resolution, the dips do not shift when ω_L is tuned across the range 1.83–1.94 eV. The off-resonance trace is dominated by doublets resembling Raman results in periodic superlattices.²⁰ As for the latter, the doublet splitting in the FSL is $\cong q\bar{c}$, where \bar{c} is the superlattice sound velocity.²⁰ In contrast to the periodic case, the centers of the doublets are not equally spaced but closely follow a *geometric* progression with τ as the common ratio. This property, implying periodicity in a logarithmic scale, reflects the self-similarity of the Fibonacci ordering.^{1-3,14,18} Other than the major doublets, the data reveal weaker lines throughout the whole spectral range. This feature relates to the dense set of δ -function peaks that characterizes the structure factor of FSL's.^{1-3,14,18}

The photoelastic continuum model²⁰ provides a basis for understanding the link between doublets and the structural properties of the FSL. The strength of the Fourier components entering in Eq. (2) is determined by the ratio of GaAs and AlAs p^{12} coefficients ($\cong 9.6$) and LA velocities ($\cong 0.82$).²⁰ Neglecting the much weaker c modulation, Eq. (2) is approximated by

$$I(\Omega(\kappa)) \propto \kappa^2 |p_{q-\kappa}|^2 [n(\Omega(\kappa)) + 1] / \Omega(\kappa), \quad (3)$$

where κ is the Bloch index. For a given P_k , Eq. (3) de-

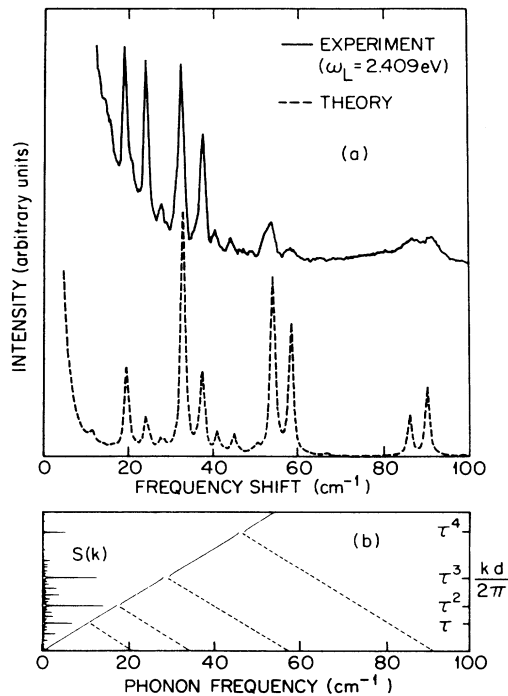


FIG. 2. (a) Comparison between measured and calculated [Eq. (2)] off-resonance spectra. (b) LA frequency vs k , and the structure factor $S(k)$. (Note that the Bloch index $\kappa = k/2$.) Largest gaps in the LA spectrum occur at $\Omega_p \cong \pi \bar{c} d^{-1} \tau^p$, with integer p . Dashed lines link Ω_p with $2\Omega_p$, giving midpositions of principal doublets.

scribes scattering by phonon doublets with $\kappa = |q \pm k|$; since the P_k 's form a dense set,¹⁻³ all modes are, in principle, allowed. In our sample, for which $d_A/d_B \cong \tau$, the largest components of the modulation (strongest features in the x-ray pattern)² correspond to $k_p = 2\pi d^{-1} \tau^p$ with integer p ($d = \tau d_A + d_B$; d_A and d_B are the thicknesses of building blocks A and B).^{1-3,14} This leads to doublets at $\Omega \cong \bar{c} |q \pm 2\pi d^{-1} \tau^p|$ accounting for the origin of the geometric progression. Calculations using the full expressions Eqs. (1) and (2) support the above approximation. The exact results, shown in Fig. 2(a), exhibit doublets only slightly shifted from the frequencies predicted by Eq. (3).

Theory and experiment are compared in Fig. 2(a). The continuum model accurately describes the positions of the Raman peaks, but not their relative intensities. This problem has also been noticed in the case of periodic superlattices.²⁰ Figure 2(b) shows the structure factor $S(k) \propto |P_k|^2$ or $|c_k|^2$ [c_k is the Fourier transform of $c(z)$] and the phonon dispersion Ω vs k ($\cong 2\kappa$) calculated from Eq. (1). The largest gaps in the spectrum correspond to $\kappa = k_p/2 = \pi d^{-1} \tau^p$. The construction to obtain the centers of doublets is also indicated: A δ function at a particular wave vector k leads to a gap at $\kappa = k/2$ and scattering at $\kappa = |q \pm k|$.

The positions of the dips in the resonant data of Fig. 1 correlate with major gaps in the 1D phonon spectrum. This is shown in Fig. 3. Based on the correlation, the scattering is ascribed to a weighted density of states of [001] LA modes. The situation here differs from the periodic counterpart in several respects. For the latter, resonances lead primarily to changes in the relative intensities of the doublets.²⁰ The development of asymmetric line shapes and interference-type behavior, as reported in Ref. 20, do not relate to our case because these effects are

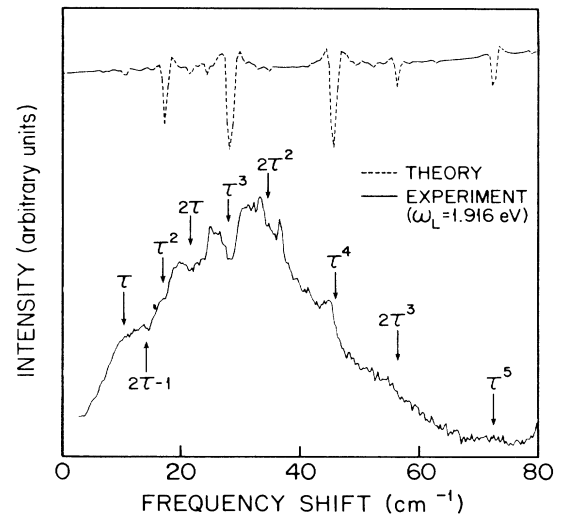


FIG. 3. The resonant spectrum after dividing by $[n(\Omega) + 1]$. Dashed curve is the calculated density of states of [001] LA modes. Arrows denote expected midfrequencies of main gaps in units of $\pi \bar{c} d^{-1}$.

strongly dependent on ω_L . Wave-vector-nonconserving scattering by zone-edge phonons^{20,21} is also unrelated; both LA and transverse-acoustic modes are involved and the doublets remain as the dominant spectral features.

The origin of the resonant scattering in Fig. 3 is not well understood. The quasiperiodicity of FSL's allows scattering by all [001] phonons, but such a general statement does not account for the differences with the nonresonant data. An interesting possibility is that the relevant electronic state is an *intrinsic* gap excitation localized at the

surface. As discussed in Ref. 12, FSL's may contain as many surface states as states of the bulk. Calculations of the electronic spectrum and further experimental work are being pursued to test this idea.

We thank P. K. Bhattacharya and F.-Y. Juang for growing the sample. This work was supported by the U.S. Army Research Office under Contracts No. DAAG-29-85-K-0175 and No. DAAL-03-86-6-0020.

-
- ¹R. Merlin, K. Bajema, R. Clarke, F.-Y. Juang, and P. K. Bhattacharya, *Phys. Rev. Lett.* **55**, 1768 (1985).
²J. Todd, R. Merlin, R. Clarke, K. M. Mohanty, and J. D. Axe, *Phys. Rev. Lett.* **57**, 1157 (1986).
³D. Levine and P. J. Steinhardt, *Phys. Rev. Lett.* **53**, 2477 (1984).
⁴M. G. Karkut, J.-M. Triscone, D. Ariosa, and Ø. Fischer, *Phys. Rev. B* **34**, 4390 (1986).
⁵A. Hu, C. Tien, X. Li, Y. Wang, and D. Feng, *Phys. Lett. A* **119**, 313 (1986).
⁶M. Kohmoto, L. P. Kadanoff, and C. Tang, *Phys. Rev. Lett.* **50**, 1870 (1983).
⁷S. Ostlund, R. Pandit, D. Rand, H. J. Schellnhuber, and E. D. Siggia, *Phys. Rev. Lett.* **50**, 1873 (1983).
⁸J. P. Lu, T. Odagaki, and J. L. Birman, *Phys. Rev. B* **33**, 4809 (1986).
⁹T. Odagaki and L. Friedman, *Solid State Commun.* **57**, 915 (1986).
¹⁰P. Hawrylak and J. J. Quinn, *Phys. Rev. Lett.* **57**, 380 (1986).
¹¹J. Kollár and A. Sütő, *Phys. Lett. A* **117**, 203 (1986).
¹²F. Nori and J. P. Rodriguez, *Phys. Rev. B* **34**, 2207 (1986).
¹³M. Kohmoto, *Phys. Rev. B* **34**, 5043 (1986).
¹⁴M. C. Valsakumar and V. Kumar, *Pramana* **26**, 215 (1986).
¹⁵M. Fujita and K. Machida, *Solid State Commun.* **59**, 61 (1986).
¹⁶S. Das Sarma, A. Kobayashi, and R. E. Prange, *Phys. Rev. B* **34**, 5309 (1986).
¹⁷Q. Niu and F. Nori, *Phys. Rev. Lett.* **57**, 2057 (1986).
¹⁸J. P. Lu and J. L. Birman, *Phys. Rev. Lett.* **57**, 2706 (1986).
¹⁹M. Kohmoto, B. Sutherland, and C. Tang, *Phys. Rev. B* **35**, 1020 (1987).
²⁰See, e.g., C. Colvard, T. A. Gant, M. V. Klein, R. Merlin, R. Fischer, H. Morkoc, and A. C. Gossard, *Phys. Rev. B* **31**, 2080 (1985), and references therein.
²¹J. Sapriel, J. Chavignon, F. Alexandre, and R. Azoulay, *Phys. Rev. B* **34**, 7118 (1986).